LETTER

CrossMark

Hikami-Larkin-Nagaoka (HLN) Treatment of the Magneto-Conductivity of Bi_2Te_3 Topological Insulator

Rabia Sultana[1,2] · Ganesh Gurjar[3] · P. Neha[3] · S. Patnaik[3] · V. P. S. Awana[1,2]

Abstract

We report the magneto-conductivity analysis at different temperatures under a magnetic field of up to 5 T of a well-characterized Bi_2Te_3 crystal. Details of crystal growth and various physical properties including high linear magneto-resistance are already reported by some of us. To elaborate upon the transport properties of Bi_2Te_3 crystal, the magneto-conductivity is fitted to the known Hikami-Larkin-Nagaoka (HLN) equation and it is found that the conduction mechanism is dominated by both surface-driven weak anti-localization (WAL) and the bulk weak localization (WL) states. The value of HLN equation coefficient (α) signifying the type of localization (WL, WAL or both WL and WAL) falls within the range of -0.5 to -1.5. In our case, the low-field (± 0.25 T) fitting of studied crystal exhibited a value of α close to -0.86 for studied temperatures of up to 50 K, indicating both WAL and WL contributions. The phase coherence length (l_φ) is found to decrease from 98.266 to 40.314 nm with increasing temperature. Summarily, the short letter reports the fact that bulk Bi_2Te_3 follows the HLN equation and quantitative analysis of the same facilitates to know the quality of studied crystal in terms of WAL to WL contributions and thus the surface to bulk conduction ratio.

Keywords Topological insulator · Magneto-resistance · Conduction mechanism

1 Introduction

Topological insulators (TIs) are the so-called wonder materials of recent times. The TIs are known to be a conventional insulator in their bulk and as a conductor at the edges/surface having gapless states, which are further protected by time reversal symmetry (TRS) [1–11]. Apart from their unique physical properties realized so far, TIs do act as challenging materials in condensed matter physics community owing to their unusual magnetic behaviour, which could possibly be used to find a variety of exotic physical phenomena resulting into novel applications. As reported, intrinsic

TIs exhibit two different types of magneto-resistance (MR) behaviour depending upon the applied magnetic field [12]. One of them is the weak anti-localization (WAL) behaviour which is observed as a typical v-type cusp (sharp MR dip) at lower magnetic field, whereas the other is the linear non-saturating MR behaviour observed at higher magnetic fields. The WAL effect exhibits negative magneto-conductivity behaviour, whereas the weak localization (WL) effect exhibits positive magneto-conductivity behaviour at lower magnetic field and temperatures. However, intrinsic TIs (Bi_2Te_3, Bi_2Se_3 and Sb_2Te_3) exhibit WAL behaviour as long as the surface state gap remains unopened but experiences a competing effect of both WAL and WL and a crossover from WAL to WL effect as the TRS is broken due to opening of a surface energy from say doping of magnetic impurities [13]. Moreover, the WAL behaviour is significantly affected depending upon the type of material such as thin film, bulk single crystals, nano-flakes and nano-wires due to size-dependent interactions between the surface and bulk states or the electron–electron interactions leading to competing WAL and WL [14–16]. It is also known that WAL behaviour is responsive only to the perpendicular component of the applied magnetic field, which is further described by the

✉ V. P. S. Awana
awana@nplindia.org
http://awanavps.webs.com

1 National Physical Laboratory (CSIR), Dr. K. S. Krishnan Road, New Delhi, 110012, India

2 Academy of Scientific and Innovative Research (AcSIR), NPL, New Delhi, 110012, India

3 School of Physical Sciences, Jawaharlal Nehru University, New Delhi, 110067, India

Hikami-Larkin-Nagaoka (HLN) model [17, 18]. The HLN model, in fact, nicely represents the surface versus bulk conduction contributions to the overall conductivity of the TIs. The two important parameters being considered in the HLN model are the pre-factor (α) and phase coherence length (l_φ). Principally, the pre-factor (α) moves from -0.5 to -1.5, depending upon the contributions from WL and WAL or the competing conduction channels. Henceforth, the fitting of magneto-conductivity of TIs to the HLN model is very fruitful to know the resultant conduction process. Additionally, the phase coherence length (l_φ) in the HLN equation is found to be temperature dependent and exhibits a power law behaviour as confirmed theoretically, i.e. $l_\varphi \sim T^{-0.5}$ for 2D systems and $l_\varphi \sim T^{-0.75}$ for 3D systems [17]. The higher the temperature, the lower the coherence length (l_φ). Recently, some of us reported detailed crystal growth and physical property characterization of one of the popular TIs, i.e. Bi_2Te_3 [19, 20]. Keeping in view the importance of the overall conduction process of a TI in terms of competing WAL and WL, in the current short article, we report the HLN treatment of the magneto-conductivity of our well-characterized [19, 20] Bi_2Te_3 single crystal.

2 Experimental Details

Bulk single crystals of Bi_2Te_3 were grown by the self-flux method via the conventional solid-state reaction route. The detailed crystal growth mechanism is illustrated in ref. [19, 20]. In brief, a stoichiometric ratio of Bi and Te powders was mixed thoroughly inside a glove box with Ar atmosphere. The mixed powder was pressed into a rectangular pellet,

sealed in an evacuated quartz tube and was kept inside an automated programmable box furnace. It was heated to 950 °C for 7.5 h, hold for 12 h and then slowly cooled (2 °C/h) to 650 °C followed by switching off the furnace. The obtained crystal was then taken out of the quartz tube and mechanically cleaved for further structural and magneto-transport measurements. The phase identification of the resultant bulk single crystal of Bi_2Te_3 was carried out using Rigaku MiniFlex II, powder X-ray diffractometer (PXRD) with Cu-Kα radiation ($\lambda = 1.5418$ Å). The magneto-transport measurements were done using a 14 T down to 2 K Quantum Design Physical Property Measurement System (PPMS), model 6000.

3 Results and Discussion

Figure 1 depicts the single-crystal XRD pattern of the resultant Bi_2Te_3 crystal in the angular range of $2\theta_{min} = 10°$ and $2\theta_{max} = 80°$. The XRD pattern shows well-indexed sharp (00l) reflections, indicating the good crystalline nature of the synthesized Bi_2Te_3 crystal. The inset (a) of Fig. 1 displays the temperature-dependent electrical resistivity plots of as-synthesized Bi_2Te_3 single crystal under different applied magnetic fields, i.e. $\rho(T)H$. The temperature varies from 5 to 50 K, whereas the applied magnetic field ranges from 0 to 6 T. Here, the resistivity curves appear to increase with temperature, clearly indicating that the as-synthesized Bi_2Te_3 single crystal exhibits a metallic nature. Further, the $\rho(T)H$ clearly shows that the resistivity increases substantially with applied field at particular temperature. The other inset of Fig. 1, i.e. inset (b), shows the percentage change

Fig. 1 X-ray diffraction pattern of as-synthesized Bi_2Te_3 single crystal. Inset (a), temperature-dependent electrical resistivity of Bi_2Te_3 single crystal in the temperature range of 5 to 50 K and magnetic field varying from 0 to 6 T. Inset (b), MR (%) as a function of magnetic field (H) perpendicular to ab plane at different temperatures for Bi_2Te_3 single crystal
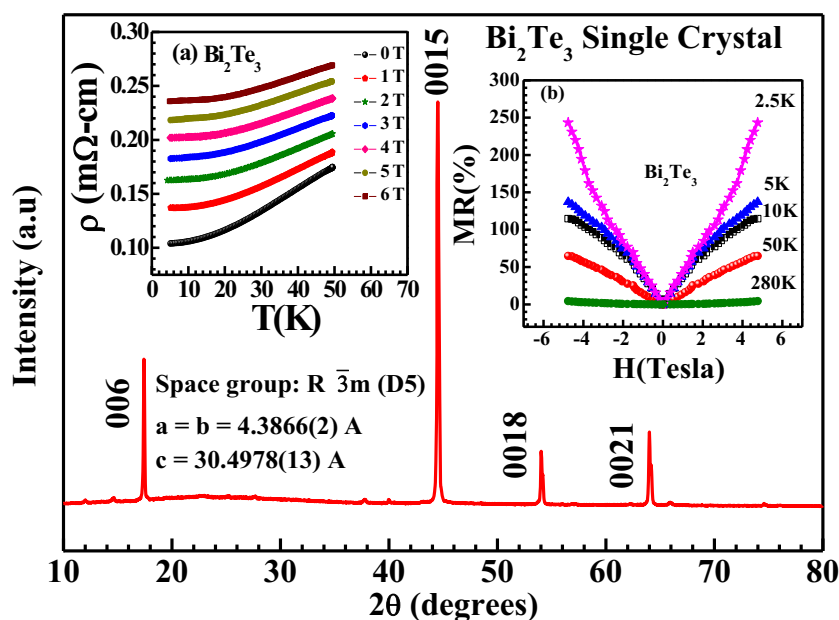
of MR under different applied magnetic fields and temperatures for the studied Bi_2Te_3 single crystal. The applied magnetic field is varied from 0 to 5 T, and the temperature ranges from 2.5 to 280 K. The MR (%) is obtained using the following formula: MR (%) = {[$\rho(H) - \rho(0)]/\rho(0)$} × 100, where $\rho(0)$ and $\rho(H)$ represent the resistivity values under zero and non-zero applied magnetic fields (H), respectively. At lower magnetic fields say below 3 T, the MR curves at 2.5, 5 and 10 K seem to overlap but bifurcate as the field is increased say above 3 T. Also, the shape of the MR curve seems to exhibit a v-type shape at the lower temperature (2.5 K) which gradually tends to broaden as the temperature is increased (5, 10 and 50 K) and finally changes into a straight line shape with least MR at the highest temperature (280 K). The calculated MR value for the lowest (2.5 K) and highest (280 K) temperatures appears to be about 250 and 5%, respectively, under a 5 T applied magnetic field. Consequently, the MR value is seen to decrease from 250% to about 5% with an increase in temperature from 2.5 to 280 K. Accordingly, we can say that the as-synthesized Bi_2Te_3 single crystal exhibits a temperature-dependent MR value under applied magnetic fields.

To study the transport properties more elaborately, we have fitted the low-field magneto-conductivity curves of the bulk Bi_2Te_3 single crystals using the HLN as below [18]

$$\Delta\sigma(H) = \sigma(H) - \sigma(0)$$
$$= -\frac{\propto e^2}{\pi h}\left[\ln\left(\frac{B_\varphi}{H}\right) - \Psi\left(\frac{1}{2} + \frac{B_\varphi}{H}\right)\right]$$

where $\Delta\sigma(H)$ represents change of magneto-conductivity, Ψ is the digamma function, e is the electronic charge, h

is Planck's constant, $B_\varphi = \frac{h}{8e\pi Hl_\varphi}$ is the characteristic magnetic field, H is the applied magnetic field, l_φ is the phase coherence length and α is a coefficient indicating the type of localization (WL, WAL or both WL and WAL). The pre-factor (α) exhibits values depending upon the type of spin-orbit interaction (SOI) and magnetic scattering [18]. Accordingly, $\alpha = 0$ when the magnetic scattering is strong (unitary case), $\alpha = 1$ when the SOI and magnetic scattering are weak or absent (orthogonal case) and $\alpha = -0.5$ when SOI is strong and there is no magnetic scattering [18].

The coefficient α, determining the type of localization as well as the number of coherent transport channels, should have values -0.5 for a single surface-conducting channel and between -0.5 and -1.5 for multi-parallel conduction channels (surface and bulk states) [21–27]. However, the experimentally fitted value of α varies widely, due to the problems arising from differentiating the bulk and surface contributions clearly. As reported, α may lie between -0.4 and -1.1, for single surface state, two surface states or intermixing between the surface and bulk states [23, 26].

Figure 2 shows the fitted magneto-conductivity curves of bulk Bi_2Te_3 single crystal and using the HLN equation at different temperatures (2.5, 5, 10 and 50 K) under applied magnetic fields of ± 2 T. Figure 2 clearly shows that at lower fields, i.e. up to ± 2 T, the magneto-conductivity curves at 2.5, 5 and 10 K seem to overlap on each other but bifurcate at higher fields and follow the HLN behaviour. However, to study the HLN equation more precisely and to extract the fitting parameters, i.e. pre-factor (α) and phase coherence length (l_φ), one need to fit the magneto-conductivity data in much lower magnetic fields, i.e. where a v-type shape is seen in MR. For this very reason in Fig. 3, we show the
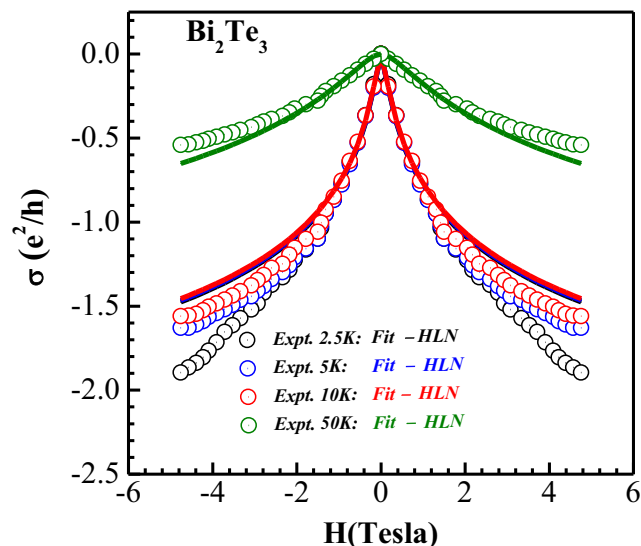

Fig. 2 WAL-related magneto-conductivity for Bi_2Te_3 single crystal at different temperatures (2.5, 5, 10 and 50 K), fitted using the HLN equation up to ± 2 T

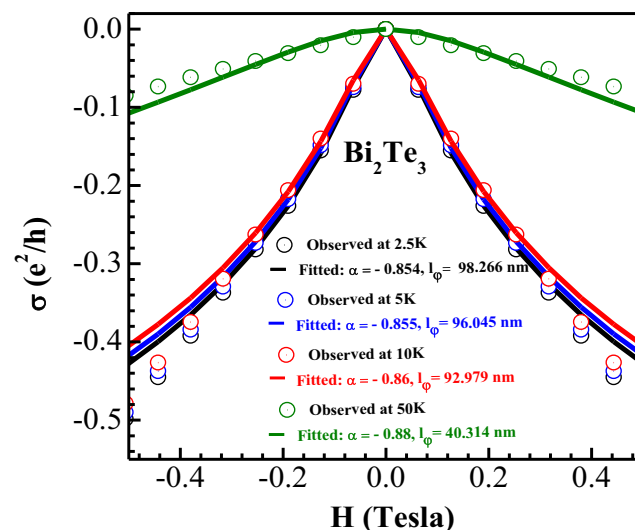**Fig. 3** Magneto-conductivity curves for Bi_2Te_3 single crystal at different temperatures (2.5, 5, 10 and 50 K), fitted using the HLN equation up to ± 0.25 T

Table 1 HLN fit values of the pre-factor (α) and phase coherence length (l_φ) for Bi_2Te_3 crystal

Temperature (K)	α	l_φ (nm)
2.5	− 0.854	98.266
5	− 0.855	96.045
10	− 0.86	92.979
50	− 0.88	40.314

HLN-fitted magneto-conductivity data of studied Bi_2Te_3 single crystal at much lower applied magnetic fields of up to ± 0.25 T. The HLN-fitted lines are indicated by solid lines, and the fitting parameters (α and l_φ) are given in the figure itself. Both α and l_φ exhibit close values of around − 0.85 and 95 nm, respectively, at lower temperatures, i.e. at 2.5, 5, and 10 K. At higher temperature, i.e. at 50 K, though the α value is close to that at lower temperatures, the phase coherence length (l_φ)) is decreased to nearly half (40 nm).

The fitted values of pre-factor (α) and phase coherence length (l_φ) at all the HLN-fitted temperatures for Bi_2Te_3 crystal are given in Table 1. It is clear from Table 1 that though the value of pre-factor (α) is nearly unchanged and remains within the range of − 0.8543 to − 0.88, the coherence length (l_φ) decrease from 92.26 to 40.31 nm at 2.5 and 50 K, respectively. At intermediate temperatures of 5 and 10 K, the α and l_φ values are − 0.85, − 0.86, and 96.04 and 92.97 nm, respectively. The resultant value of α at studied temperatures, i.e. at 2.5, 5, 10 and 50 K, of around − 0.8543 to − 0.88 demonstrates that the conduction mechanism is dominated by both WAL and WL as being originated from both the 2D surface and 3D bulk states of the studied TI [27, 28]. Further, at 50 K, the relatively lower value of coherence length (40.314 nm) indicates the more dominance of WL over WAL. It is clear that our quality bulk Bi_2Te_3 crystal follows the HLN equation. The HLN analysis could be a fruitful exercise to know the quality of the topological insulators in terms of surface-to-bulk conduction ratio.

Summarily, we analysed the magneto-conductivity data of our quality Bi_2Te_3 bulk single crystal in terms of the HLN equation and found that both the WAL and WL contribute to the conduction process. Further, it is seen that phase coherence length decreases to nearly half from around 98 to 40 nm as the temperature increased from 2.5 to 50 K.

References

1. Kane, C.L., Mele, E.J.: Phys. Rev. Lett. **95**, 146802 (2005)
2. Bernevig, B.A., Zhang, S.-C.: Phys. Rev. Lett. **96**, 106802 (2006)
3. Fu, L., Kane, C.L., Mele, E.J.: Phys. Rev. Lett. **98**, 106803 (2007)
4. Hasan, M.Z., Kane, C.L.: Rev. Mod. Phys. **82**, 3045 (2010)
5. Moore, J.E.: Nature **464**, 194 (2010)
6. Qi, X.L., Zhang, S.C.: Rev. Mod. Phys. **83**, 1057 (2011)
7. Roushan, P., Seo, J., Parker, C.V., Hor, Y.S., Hsieh, D., Qian, D., Richardella, A., Hasan, M.Z., Cava, R.J., Yazdani, A.: Nature **460**, 1106 (2009)
8. Chen, Y.L., Chu, J.-H., Analytis, J.G., Liu, Z.K., Igarashi, K., Kuo, H.-H., Qi, X.L., Mo, S.K., Moore, R.G., Lu, D.H., Hashimoto, M., Sasagawa, T., Zhang, S.C., Fisher, I.R., Hussain, Z., Shen, Z.X.: Science **329**, 659 (2010)
9. Liu, Q., Liu, C.X., Xu, C., Qi, X.-L., Zhang, S.-C.: Phys. Rev. Lett. **102**, 156603 (2009)
10. Abanin, D.A., Pesin, D.A.: Phys. Rev. Lett. **106**, 136802 (2011)
11. Qi, X.-L., Hughes, T.L., Zhang, S.-C.: Phys. Rev. B **78**, 195424 (2008)
12. Wang, Z.H., Yang, L., Zhao, X.T., Zhang, Z.D., Gao, X.P.A.: Nano Res. **8**, 2963 (2015)
13. Lu, H.-Z., Shi, J., Shen, S.-Q.: Phys. Rev. Lett. **107**, 076801 (2011)
14. Garate, I., Glazman, L.: Phys. Rev. B **86**, 035422 (2012)
15. Lu, H.-Z., Shen, S.-Q.: Phys. Rev. Lett. **112**, 146601 (2014)
16. Adroguer, P., Liu, W.E., Culcer, D., Hankiewicz, E.M.: Phys. Rev. B **92**, 241402 (2015)
17. Bao, L., He, L., Meyer, N., Kou, X., Zhang, P., Chen, Z.-G., Fedorov, A.V., Zou, J., Riedemann, T.M., Lograsso, T.A., Wang, K.L., Tuttle, G., Xiu, F.: Sci. Rep. **2**, 726 (2012)
18. Hikami, S., Larkin, A.I., Nagaoka, Y.: Prog. Theor. Phys. **63**, 707 (1980)
19. Sultana, R., Neha, P., Goyal, R., Patnaik, S., Awana, V.P.S.: J. Magn. Mag. Mater. **428**, 213 (2017)
20. Sultana, R., Gurjar, G., Patnaik, S., Awana, V.P.S.: Mat. Res. Exp. **5**, 046107 (2018)
21. He, H.T., Wang, G., Zhang, T., Sou, I.K., Wong, G.K., Wang, J.N.: Phys. Rev. Lett. **106**, 166805 (2011)
22. Ning, W., Du, H., Kong, F., Yang, J., Han, Y., Tian, M., Zhang, Y.: Sci. Rep. **3**, 1564 (2013)
23. Cha, J.J., Kong, D., Hong, S.-S., Analytis, J.G., Lai, K., Cui, Y.: Nano Lett. **12**, 1107 (2012)
24. Hamdou, B., Gooth, J., Dorn, A., Pippel, E., Nielsch, K.: Appl. Phys. Lett. **102**, 223110 (2013)
25. Akiyama, R., Fujisawa, K., Yamaguchi, T., Ishikawa, R., Kuroda, S.: Nano Res. **9**, 490 (2016)
26. Lu, H.Z., Shen, S.Q.: Phys. Rev. B **84**, 125138 (2011)
27. Bao, L., Wang, W., Meyer, N., Liu, Y., Zhang, C., Wang, K., Ai, P., Xiu, F.: Sci. Rep. **3**, 2391 (2013)
28. Liu, M., Zhang, J., Chang, C.Z., Zhang, Z., Feng, X., Li, K., He, K., Wang, L.L., Chen, X., Dai, X., Fang, Z., Xue, Q.-K., Ma, X., Wang, Y.: Phys. Rev. Lett. **108**, 036805 (2012)